

## MIT Open Access Articles

*Helminth co-infection in Helicobacter pylori infected INS-GAS mice attenuates gastric premalignant lesions of epithelial dysplasia and glandular atrophy and preserves colonization resistance of the stomach to lower bowel microbiota*

The MIT Faculty has made this article openly available. **Please share** how this access benefits you. Your story matters.

**Citation:** Whary, Mark T., Sureshkumar Muthupalani, Zhongming Ge, Yan Feng, Jennifer Lofgren, Hai Ning Shi, Nancy S. Taylor, et al. "Helminth Co-Infection in Helicobacter Pylori Infected INS-GAS Mice Attenuates Gastric Premalignant Lesions of Epithelial Dysplasia and Glandular Atrophy and Preserves Colonization Resistance of the Stomach to Lower Bowel Microbiota." *Microbes and Infection* 16, no. 4 (April 2014): 345–55.

**As Published:** <http://dx.doi.org/10.1016/j.micinf.2014.01.005>

**Publisher:** Elsevier

**Persistent URL:** <http://hdl.handle.net/1721.1/99365>

**Version:** Author's final manuscript: final author's manuscript post peer review, without publisher's formatting or copy editing

**Terms of use:** Creative Commons Attribution



Published in final edited form as:

*Microbes Infect.* 2014 April ; 16(4): 345–355. doi:10.1016/j.micinf.2014.01.005.

## Helminth co-infection in *Helicobacter pylori* infected INS-GAS mice attenuates gastric premalignant lesions of epithelial dysplasia and glandular atrophy and preserves colonization resistance of the stomach to lower bowel microbiota

Mark T. Whary<sup>\*,a</sup>, Sureshkumar Muthupalani<sup>a</sup>, Zhongming Ge<sup>a</sup>, Yan Feng<sup>a</sup>, Jennifer Lofgren<sup>a</sup>, Hai Ning Shi<sup>b</sup>, Nancy S. Taylor<sup>a</sup>, Pelayo Correa<sup>c</sup>, James Versalovic<sup>d</sup>, Timothy C. Wang<sup>e</sup>, and James G. Fox<sup>a</sup>

<sup>a</sup>Division of Comparative Medicine, Massachusetts Institute of Technology, Cambridge, MA, USA

<sup>b</sup>Mucosal Immunology Laboratory, Massachusetts General Hospital and Harvard Medical School, Boston, MA, USA

<sup>c</sup>Department of Medicine, Vanderbilt University School of Medicine, Nashville, Tennessee, USA

<sup>d</sup>Department of Pathology, Baylor College of Medicine and Texas Children's Hospital, Houston, TX, USA

<sup>e</sup>Division of Digestive and Liver Disease, Columbia University Medical Center, New York, NY, USA

### Abstract

Higher prevalence of helminth infections in *H. pylori* infected children was suggested to potentially lower the life-time risk for gastric adenocarcinoma. In rodent models, helminth co-infection does not reduce *Helicobacter*-induced inflammation but delays progression of pre-malignant gastric lesions. Because gastric cancer in INS-GAS mice is promoted by intestinal microflora, the impact of *Heligmosomoides polygyrus* co-infection on *H. pylori*-associated gastric lesions and microflora were evaluated. Male INS-GAS mice co-infected with *H. pylori* and *H. polygyrus* for 5 months were assessed for gastrointestinal lesions, inflammation-related mRNA expression, FoxP3<sup>+</sup> cells, epithelial proliferation, and gastric colonization with *H. pylori* and Altered Schaedler Flora. Despite similar gastric inflammation and high levels of proinflammatory mRNA, helminth co-infection increased FoxP3<sup>+</sup> cells in the corpus and reduced *H. pylori*-associated gastric atrophy (p<0.04), dysplasia (p<0.02) and prevented *H. pylori*-induced changes in the gastric flora (p<0.05). This is the first evidence of helminth infection reducing *H. pylori*-induced gastric lesions while inhibiting changes in gastric flora, consistent with prior observations that gastric colonization with enteric microbiota accelerated gastric lesions in INS-GAS mice.

© 2014 Elsevier Masson SAS. All rights reserved.

\*Corresponding Author: Mark T Whary, 77 Mass Ave 16-825A, Cambridge, MA 02139, 617-253-9435, FAX 617-258-5708, mwhary@mit.edu.

**Publisher's Disclaimer:** This is a PDF file of an unedited manuscript that has been accepted for publication. As a service to our customers we are providing this early version of the manuscript. The manuscript will undergo copyediting, typesetting, and review of the resulting proof before it is published in its final citable form. Please note that during the production process errors may be discovered which could affect the content, and all legal disclaimers that apply to the journal pertain.

Identifying how helminths reduce gastric premalignant lesions and impact bacterial colonization of the *H. pylori* infected stomach could lead to new treatment strategies to inhibit progression from chronic gastritis to cancer in humans.

## Keywords

*Helicobacter pylori*; *Heligmosomoides polygyrus*; Altered Schaedler Flora; INS-GAS mice; gastric cancer

## 1. Introduction

Chronic *Helicobacter pylori*-induced gastritis in humans can progress to gastric atrophy, intestinal metaplasia and dysplasia with increased risk for gastric adenocarcinoma [1]. Epidemiologic evidence in humans and data from rodent models support that gastric carcinogenesis is multifactorial, influenced by host genetics [2], hormones [3], *H. pylori* virulence properties [4], environmental co-factors [5, 6] and co-infections with enterohepatic *Helicobacters* [7, 8] or helminths [9]. Higher prevalence of helminth infections in *H. pylori* infected children was suggested to potentially lower the life-time risk for gastric adenocarcinoma [9], with serologic evidence that life-long exposure through adulthood to a variety of parasites impacts inflammatory responses to *H. pylori* [10]. Experimental data from rodent models further support this hypothesis: gastric atrophy was reduced in *H. felis* and *Heligmosomoides polygyrus* co-infected C57BL/6 mice [11] and in *H. pylori* and *Brugia pahangi* co-infected gerbils [12].

Notably in rodent models, helminth co-infection does not reduce *Helicobacter*-induced inflammation but does delay progression of pre-malignant lesions, suggesting these lesions are suppressed by an alternative mechanism not directly related to severity of the inflammatory response. Evidence from human patients [13, 14] supports that gastric cancer risk may be promoted by enteric microbiota colonizing the gastric epithelium as a sequela to *H. pylori*-induced gastric atrophy and hypochlorhydria. Recent results from rodent models reinforce the potential importance of non-*H. pylori* bacteria in accelerating gastric pathology [15][16]. Transgenic INS-GAS mice, particularly males [17-19], develop hypergastrinemia, gastric hyperplasia of the foveolar and glandular epithelium, loss of chief and parietal cells (hypochlorhydric atrophy) and severe dysplasia of gastric glands that can invade through the muscularis mucosa of the corpus. Lesion progression was delayed by months in gnotobiotic INS-GAS mice monoassociated with *H. pylori* compared to INS-GAS mice that commonly develop intraepithelial neoplasia [20] when colonized with *H. pylori* and complex (normal) enteric microbiota [15]. Additional experiments demonstrated that gnotobiotic INS-GAS colonized with *H. pylori* and a restricted, select set of 3 members of Altered Schaedler Flora (ASF 356 *Clostridium sp.*, ASF 361 *Lactobacillus sp.*, ASF 519 *Bacteroides sp.*), developed gastritis and premalignant gastric lesions equivalent to *H. pylori* infected INS-GAS mice with complex microflora (e.g. specific pathogen free mice)[16]. These results support prior findings that chronic oral administration of proton pump inhibitors to achieve gastric hypochlorhydria in *H. pylori*-infected gerbils promoted the progression of atrophic corpus gastritis to adenocarcinoma [21, 22].

These studies in rodents and observations that gastric cancer patients were found to be colonized with bacteria from 5 other bacterial phyla in addition to *H. pylori* [23], suggest colonization efficiency, rather than pathogenic potential, of specific lower bowel microflora is an important contributor to gastric cancer development. Because *H. polygyrus* prevented gastric atrophy in C57BL/6 mice co-infected with *H. felis* [11] and promoted levels of probiotic-type bacteria in the proximal intestine of mice [24], we assessed potential changes in gastric bacterial colonization in *H. pylori* and *H. polygyrus* co-infected male INS-GAS mice at 5 months post *H. pylori* infection when gastric atrophy in this model is well established.

## 2. Materials and methods

### 2.1. Infection models

**2.1.1. Mouse model**—Male, transgenic INS-GAS mice on a FVB/N background (Tg (Ins1-GAS) 1Sbr) [25] were produced by in-house breeding and maintained specific pathogen-free (SPF) of exogenous murine viruses, pathogenic bacteria (including *Helicobacter*) and ecto- and endoparasites. Mice were housed in an Association for Assessment and Accreditation of Laboratory Animal Care-accredited facility under environmental conditions of a 12:12 light / dark cycle, temperature maintenance at  $20 \pm 1^\circ\text{C}$  and relative humidity range of 30-70%. Mice were group housed in microisolator caging on hardwood bedding and provided reverse osmosis water and pelleted diet (ProLab 2000, Purina Mills, St. Louis, MO) *ad libitum*. Animal use was approved by the MIT Committee on Animal Care.

**2.1.2. Experimental infection with *Heligmosomoides polygyrus***—*H. polygyrus* were cultivated and prepared for dosing as previously described [26]. At 6 weeks of age, 23 male INS-GAS mice were orally dosed with 200 third stage (L3) *H. polygyrus* larvae in 200  $\mu\text{l}$ . At 9 and 14 days post infection, mice were treated orally with 172 mg/kg of pyrantel pamoate (Apothecary Products, Minneapolis, MN) in 200  $\mu\text{l}$  to eliminate adult parasites from the intestine. Mice were re-infected with 200 L3 larvae 1 week and 4 months following the first pyrantel pamoate dosing to mimic chronic exposure to helminths. Persistent infection with *H. polygyrus* was confirmed by elevated serum IgE levels at 2, 3 and 4 months post infection (mpi), observation of adult worms at necropsy, and histologic evidence of multiple life stages in the duodenum.

**2.1.3. Experimental infection with *Helicobacter pylori***—At 10 weeks of age, 10 of the *H. polygyrus* infected and 13 naïve male, INS-GAS mice were orally gavaged with  $1 \times 10^8$  colony forming units of *H. pylori* SS1 in 200  $\mu\text{l}$  every other day for a total of 3 doses. Controls included 9 non-dosed, uninfected mice and 13 mice infected with *H. polygyrus* alone. Persistent infection with *H. pylori* was confirmed by quantitative PCR (qPCR) of gastric tissues [8].

### 2.2. Necropsy

Mice were euthanized with carbon dioxide and necropsied at 5 mpi with *H. pylori* except for 3 *H. pylori* and *H. polygyrus* co-infected mice that were evaluated at 4 mpi to evaluate

progression of pathology and infection with *H. pylori* and *H. polygyrus*. The stomach was incised along the greater curvature and individual linear gastric strips from lesser curvature of the gastric cardia into the proximal duodenum were collected. These were either fixed in formalin or were flash-frozen in liquid nitrogen and subsequently stored at -80°C pending RNA and DNA extraction to quantify mRNA expression and colonization levels of *H. pylori* and 8 ASF using qPCR. Tissues fixed in 10% buffered formalin were paraffin embedded and 5 µm sections were processed routinely for histology and immunohistochemistry.

**2.2.1. Lesion scoring**—Tissue sections were scored for gastric lesions using previously published criteria [6] by a board certified veterinary pathologist (S.M.) blinded to sample identity. Briefly, pathology subfeatures of the gastric corpus, including inflammation (extent of inflammatory infiltrates into the mucosa and submucosa), epithelial defects (degeneration of the surface epithelium and underlying glands), mucous metaplasia, hyalinosis, epithelial hyperplasia (elongation of gastric glands lined by foveolar and glandular lining cells), pseudopyloric metaplasia (abnormal mucosa resembling pyloric antrum in glandular phenotype and mucin expression, analogous to findings in *H. pylori* infected humans), oxyntic gland atrophy (loss of chief and parietal cells) and dysplasia (based on a combination of the extent of glandular architectural distortion and degree of cellular atypia) were evaluated and graded on an ascending scale from 0 to 4. For all categories, an increment of 0.5 was used in some instances when the degree of histological changes was considered to fall between two grades represented by ordinal values. Dysplastic / neoplastic changes were graded as low (score= 1), moderate (score= 2), high (score=3, non-invasive high grade dysplasia, carcinoma *in situ*), or invasive neoplasms (score of 3.5 or 4). A score of 3.5 represented intramucosal carcinoma with invasion into lamina propria or muscularis mucosa and a score of 4 was assigned to submucosal carcinoma or beyond. Both invasive and non-invasive high grade dysplasia/gastrointraepithelial neoplasia- type (GIN) lesions were considered to be gastric cancers similar to that described in human literature [27, 28]. Differentiation of truly invasive glands from glandular herniation or pseudoinvasion into the submucosa in the murine gastrointestinal tract can be problematic and the guidelines established by Boivin et. al. [20] were specifically followed in this study for histological evaluation of the stomach. Excluding mucous metaplasia and hyalinosis which can occur independent of *H. pylori* infections, the scores for all other sub-feature categories were totaled to represent a gastric histopathologic activity index (GHAI) with a maximum possible score of 24 [6].

**2.2.2. Immunohistochemistry**—Immunohistochemistry was performed to phenotype Ki67<sup>+</sup> and FoxP3<sup>+</sup> cells in the gastric mucosa of 5 to 7 INS-GAS mice from each infection or control group at 5 mpi using previously described methods for antigen retrieval, blocking steps and counterstaining [29]. Formalin-fixed gastric sections were stained for the regulatory T cell marker FoxP3 using the FJK-16S antibody (eBiosciences, San Diego, CA) and nuclear cell proliferation marker Ki67 using mouse anti-human antibody (#550609 BD Biosciences), with color development using the #K3954 Dako Art kit (Dako, Carpinteria, CA) per instructions. For assessment of epithelial cell proliferation lining the gastric glands, Ki67 labeling indices were calculated (using a 40× microscope objective lens) by the number of positively stained nuclei per distinct linear gastric gland averaged over 10 well-

oriented glands in the gastric corpus. At the same magnification, cells expressing FoxP3<sup>+</sup> in the gastric corpus were counted and averaged over 10 representative fields of the gastric mucosa and submucosa. Nuclear labeling was considered specific for regulatory T cells, whereas granular cytoplasmic staining of oxyntic cells, if any, was considered as nonspecific background staining.

### 2.3. mRNA expression levels of cytokines and iNOS

mRNA expression levels in gastric sections were measured by qPCR as previously described [15]. Total RNA from flash-frozen gastric tissue was extracted with Trizol reagent (Invitrogen, Carlsbad, CA) and cDNA synthesized from 5 µg of total RNA using the High Capacity cDNA Archive kit (Applied Biosystems). mRNA levels for IL-10, TGFβ, IL-17A, IL-17F, IL-1β, TNFα, IFNγ, iNOS, and GAPDH (endogenous control) were quantified using TaqMan gene expression assays (Applied Biosystems, Foster City, CA) in the 7500 FAST Sequence Detection System. mRNA levels were normalized to GAPDH expression with baseline comparisons made to uninfected mice using the CT method (User Bulletin #2, Applied Biosystems) as previously described [15].

### 2.4 Colonization levels of *H. pylori* and Altered Schaedler Flora

DNA was extracted from the stomach using the High Pure PCR Template Preparation Kit (Roche Molecular Biochemicals, Indianapolis, IN). As previously published, samples were probed with 18S rRNA-based primers for quantifying mouse DNA (Applied Biosystems) and with *H. pylori* DNA-specific primers and probe based on the *H. pylori ureB* gene [8]. ASF copy numbers were measured using SyBr-based qPCR using the 7500 Fast Sequence Detection System (Applied Biosystems) [30, 31]. Plasmid DNA containing the 16S rDNA of each of the 8 ASF species was used to generate standard curves of six 10-fold dilutions, ranging from 10<sup>6</sup> to 10 copies. Subsequently, the bacterial DNA quantity was converted into copy number of each ASF genome based on the number of 16S rRNA gene copies. ASF copy numbers were then normalized to µg of mouse chromosomal DNA.

### 2.5 ELISA for serum IgE response to *H. polygyrus*

Five randomly selected mice from each experimental group were bled at 2, 3 and 4 months post *H. polygyrus* dosing to monitor serum IgE levels in response to helminth infection as previously described [32]. The ELISA plates were coated with rat anti-mouse antibody to IgE (BD Biosciences, Franklin Lakes NJ), incubated with diluted sera, and IgE detected with biotin-conjugated rat anti-mouse IgE (BD Biosciences) and peroxidase-conjugated streptavidin (Invitrogen). Optical density values developed with *O*-phenylenediamine at 492 nm were converted to ng/ml of IgE by comparison with a standard curve of purified IgE (BD Biosciences) by linear regression analysis, and are expressed as the mean concentration for each group of mice ± standard deviation.

### 2.6 Statistical analysis

Except for gastric lesion scores, all other data analyzed statistically were from mice necropsied at a time point equivalent to 5 mpi with *H. pylori*. Gastric lesion scores were combined from mice necropsied at both 4 and 5 mpi because scores were statistically

equivalent. Data analysis for GHAI, subfeature lesion scores, Ki67 and FoxP3 immunohistochemistry were compared using the Mann-Whitney nonparametric test. The Fishers exact test was used to evaluate the incidence and odds ratio of developing GIN. Cytokine and iNOS mRNA expression levels and log-transformed qPCR colonization data for *H. pylori* and ASF were evaluated using the Student t test. Statistical analysis was performed using GraphPad Prism 5.0 (GraphPad Software, Inc., La Jolla, CA). Results were considered significant at  $p < 0.05$ .

### 3. Results

#### 3.1. Heligmosomoides polygyrus infection caused persistent inflammatory responses

INS-GAS mice were infected with L3 stage *H. polygyrus*, treated with an anthelmintic and orally redosed with larvae two additional times. Multiple life stages of *H. polygyrus* were observed grossly at necropsy (adult worms) and in histologic sections of the duodenum (degenerate larvae and adults) (not shown). The majority of *H. polygyrus* infected mice developed duodenitis ranging from mild neutrophilic infiltration to severe mural-serosal, pyogranulomatous lesions, consisting of neutrophilic and mononuclear inflammation in response to degenerate and necrotic nematodes in the wall of the small intestine. As additional evidence of chronic immune stimulation from *H. polygyrus*, the total mean  $\pm$  standard deviation of serum IgE levels in *H. polygyrus* infected mice were  $166 \pm 82$  ng/ml,  $179 \pm 82$  ng/ml in *H. pylori* and *H. polygyrus* coinfecting mice, compared to significantly lower levels in mice infected with *H. pylori* alone ( $19 \pm 28$  ng/ml) ( $p < 0.002$ ).

#### 3.2. Co-infection with Heligmosomoides polygyrus reduced premalignant and malignant gastric lesions in Helicobacter pylori infected INS-GAS mice

Control, uninfected INS-GAS mice or mice infected with *H. polygyrus* alone had similar gastric histopathologic activity indices (median and range GHAI of 8 (6.5-9.5) for controls; 8.5 (6-10.5) for *H. polygyrus* alone) with low to moderate severity scores for subfeatures of gastritis, epithelial defects, foveolar hyperplasia, glandular atrophy, pseudopyloric metaplasia and dysplasia (Fig. 1A-F, 2A-H). In the absence of *H. pylori* infection, lesions consisted mainly of foveolar hyperplasia (Fig. 1C, 2B) and early dysplasia (Fig. 1F, 2B) that were attributable to hypergastrinemia as previously reported [15, 19].

Compared to controls, INS-GAS mice mono-infected with *H. pylori* developed gastritis that was most severe in the corpus (Fig. 1A, 2C). *H. pylori* infected mice had higher GHAI (median and range GHAI of 16 (14-18) compared to uninfected controls (8 (6.5-9.5);  $p < 0.0001$ ) attributable to significantly greater inflammation, epithelial defects, hyperplasia, atrophy, metaplasia and dysplasia (Fig. 2A-F) ( $p < 0.0002$ ). INS-GAS mice infected with *H. pylori* had significant distortion of normal gastric architecture with cystic mucous metaplasia of glands in the corpus (Fig. 2C-D), epithelial defects, hyperplasia, oxyntic atrophy, pseudopyloric metaplasia and dysplasia, accompanied by edema and mild inflammatory infiltrates in the submucosa (Fig. 2C-F). High grade dysplastic glands frequently contained necrotic, apoptotic cellular debris (Fig. 2E) and in some instances exhibited budding nests of invasive cells in the lamina propria consistent with the diagnosis of intramucosal carcinoma (dysplasia score of 3.5). Occasionally, one or more dysplastic glandular units were seen

either partially or fully extending vertically down into the submucosa. Close examination confirmed the presence of a discernible peripheral muscularis mucosa and so these lesions were considered as herniated glands or pseudoinvasion, a frequent finding in mouse GI tracts which must be differentiated on the basis of true invasion [20] (Fig. 2F). Notably, 8 of 12 male INS-GAS mice infected with *H. pylori* alone developed non-invasive neoplasms and 2 of 12 mice developed invasion of dysplastic glands into the lamina propria, fulfilling the definition of intramucosal carcinomas (Fig. 2E).

Compared to mice mono-infected with *H. pylori*, INS-GAS mice co-infected with *H. pylori* and *H. polygyrus* had similar degrees of inflammation, epithelial defects, hyperplasia and pseudopyloric metaplasia (Fig. 2A-E). Immunolabeling for Ki67, a marker of epithelial cell proliferation, supported lesion scoring of hematoxylin and eosin-stained sections that *H. pylori* infection resulted in significant epithelial hyperplasia ( $p < 0.004$ ) that was not reduced by *H. polygyrus* co-infection (Fig. 3A). Notably however, gastric atrophy ( $p < 0.04$ ) and dysplasia ( $p < 0.02$ ) were reduced by *H. polygyrus* co-infection (Fig. 1D, 1F and 2H). Non-invasive high grade dysplasia was evident in only 4 of 10 co-infected mice and none had developed invasive neoplasms (intramucosal carcinoma or submucosal carcinoma) (Fig. 1F). Although herniation of dysplastic glands was noted in mice infected with *H. pylori* and in mice co-infected with *H. polygyrus*, the extent of herniation and degree of cytological atypia were greater in the *H. pylori* infected mice. The odds ratio for developing GIN in mice mono-infected with *H. pylori* was 11.7 ( $p < 0.03$ ; 95% CI 1.5-89.2) compared to mice co-infected with *H. pylori* and *H. polygyrus*.

### 3.3. FoxP3<sup>+</sup> cells were elevated in number in the gastric lamina propria of INS-GAS mice co-infected with *H. pylori* and *H. polygyrus*

Immunohistochemistry labeling for the regulatory T cell marker FoxP3 demonstrated that the gastric tissues from *H. pylori* infected INS-GAS mice contained significantly elevated numbers of FoxP3<sup>+</sup> regulatory T cells compared to uninfected controls or mice infected with *H. polygyrus* alone ( $p < 0.01$ ) (Fig. 6B). Gastric tissues from INS-GAS mice co-infected with *H. pylori* and *H. polygyrus* contained statistically higher numbers of FoxP3<sup>+</sup> regulatory T cells than mice mono-infected with *H. pylori* ( $p < 0.03$ ).

### 3.4. Cytokine and iNOS mRNA responses to *H. pylori* were unaffected by co-infection with *H. polygyrus*

Mice mono-infected with *H. pylori* developed robust (15 to 100+ fold) mRNA expression levels in the gastric corpus for proinflammatory IFN- $\gamma$ , IL-17F, IL-17A, TNF $\alpha$ , and iNOS (all  $p < 0.0001$ ) (Table 1). Mice co-infected with *H. polygyrus* and *H. pylori* developed similar, elevated levels of proinflammatory gene expression that were equivalent to levels observed in mice infected with *H. pylori* alone. Proinflammatory IL-1 $\beta$  and anti-inflammatory TGF $\beta$  and IL-10 mRNA expression levels were statistically elevated by *H. pylori* and *H. pylori* / *H. polygyrus* co-infection ( $p < 0.05$ ) but were orders of magnitude lower than the expression levels of the pro-inflammatory genes. IL-13 expression was also assessed but mRNA levels were at background levels. The duodenitis noted in *H. polygyrus* challenged mice did not alter expression of proinflammatory genes in the corpus as mRNA



levels were similar between mice infected with *H. polygyrus* alone and uninfected control mice.

By qPCR assay, gastric colonization of *H. pylori* was not detected in 2 of 12 mice dosed with *H. pylori* alone (Fig. 4) which is attributable to gastrin-associated gastritis that is further promoted by *H. pylori* infection. Gastric lesions in these mice were similar to the other mice mono-infected with *H. pylori*: therefore, data on these mice were included in the 5 mpi analysis. Gastric colonization levels of *H. pylori* were similar in the remaining *H. pylori* infected mice irrespective of co-infection with *H. polygyrus*. Seven of 8 ASF species were detected by qPCR in gastric samples; the extremely oxygen-sensitive ASF 492, which clusters taxonomically with *Eubacterium plexicaudatum* [33] was undetectable in all samples. *H. pylori* infection promoted gastric colonization levels of 4 of the 7 ASF species (ASF 356 *Clostridium* sp., ASF 361 *Lactobacillus* sp., ASF 457 *Mucispirillum schaedleri*, ASF 500 *Clostridium* sp.) by approximately 1 log ( $p < 0.02$ ), whereas *H. polygyrus* co-infection prevented increased gastric colonization with 3 of these same ASF (ASF 356, ASF 457 and ASF 500) ( $p < 0.05$ ). Colonization levels observed in *H. pylori* and *H. polygyrus* co-infected mice were comparable to uninfected control mice (Fig. 4). Colonization of ASF 360 *Lactobacillus* sp., ASF 502 *Clostridium* sp. and ASF 519 *Bacteroides* sp. were at levels comparable to the other detectable ASF but their colonization levels were unaffected by either *H. pylori* or *H. polygyrus* infection.

#### 4. Discussion

As previously reported, *H. pylori* infection in male INS-GAS mice caused gastritis, foveolar hyperplasia, gastric atrophy, pseudopyloric metaplasia and progression of chronic gastritis to invasive gastrointraepithelial neoplasia (GIN) [17, 19]. GIN was first described for lower bowel carcinomas in rodents [20] and has histologic features compatible with gastric adenocarcinoma in humans [34]. The increase in gastric colonization with ASF in *H. pylori* infected INS-GAS mice supports the hypothesis that lower bowel microflora may contribute to gastric carcinogenesis in humans. *H. polygyrus* co-infection modulated both of these features; gastric atrophy, dysplasia and the incidence of invasive GIN were reduced and colonization resistance of the stomach to ASF was maintained.

Dysplasia leads to non-invasive and invasive neoplasms. GIN is equivalent to high grade dysplasia. The results from the current study demonstrate that *H. polygyrus* infection reduced gastric atrophy and dysplasia, and in particular, reduced the extent of dysplastic glands invading through the muscularis mucosa into the lamina propria. The odds ratio for developing GIN in mice infected with *H. pylori* alone was significantly elevated compared to mice co-infected with *H. pylori* and *H. polygyrus*. Consistent with prior data on helminth and *Helicobacter* co-infection in mice [11] and in gerbils [12], *H. polygyrus* co-infection did not reduce gastric inflammation. Thus, in three rodent models, helminthiasis reduced *Helicobacter*-associated gastric atrophy without reduction in gastric inflammation per se, supporting the hypothesis that *H. pylori*-associated premalignant gastric lesions are prevented, at least in part, by an alternative mechanism not directly related to severity of gastric inflammation.

Although ASF have historically been used to colonize germfree mice with a defined flora to establish normal gut physiology and to establish commercially-reared mice under SPF conditions, phylogenetic classification of these 8 anaerobes based on 16SrRNA taxonomy [33] and spatial distribution within the mouse gastrointestinal tract [30] are relatively recent. Little is known about the long-term impact on gut physiology or pathogenic potential of the 8 member species of ASF. Acknowledging that gastric colonization with various other bacterial species may have increased or decreased secondary to *H. pylori* or *H. polygyrus* infection, ASF were used in this study to monitor microbial population shifts in gastric bacteria as we have previously demonstrated altered population dynamics in the lower bowel after infection with *H. trogonatum* in C57BL/6 IL-10<sup>-/-</sup> mice [35] and in outbred Swiss mice infected with *H. hepaticus* [31]. The increase in gastric colonization with ASF in *H. pylori* infected INS-GAS mice supports the hypothesis that lower bowel microflora may contribute to gastric carcinogenesis in humans. The potential role for enteric bacteria not typically associated with gastric disease to promote *H. pylori*-associated gastritis and gastric cancer is also supported by our previous observations. Although *H. pylori* as a mono-infection caused gastritis in gnotobiotic INS-GAS mice, lesions were less severe in comparison to *H. pylori* infected SPF INS-GAS mice with a complex enteric microbiota under otherwise similar experimental conditions [15]. We also recently demonstrated that gnotobiotic INS-GAS mice colonized with just 3 members of ASF replicated the promotion of neoplastic lesions by diverse intestinal flora in the *H. pylori* INS-GAS mouse model [16].

In this current study, 4 ASF species colonized the *H. pylori* infected stomach at significantly higher levels and suggests that parietal cell loss from chronic inflammation and subsequent increase in gastric pH enables a variety of enteric bacteria to colonize the hypochlorhydric stomach, as shown in *H. pylori* infected INS-GAS mice in which members of the *Bacteroidetes* phyla were reduced and *Firmicutes* phyla were increased in the stomach compared to uninfected INS-GAS mice [15]. Similarly, gastric bacterial overgrowth occurs in mice with genetic or chemically induced hypochlorhydria [36] and chronic dosing of proton pump inhibitors that increase gastric pH in *H. pylori* infected gerbils promoted the progression of atrophic corpus gastritis to adenocarcinoma [21, 22]. Opportunistic bacteria could further drive inflammatory responses in the stomach, accelerating atrophy and dysplasia by means of mutagenic properties or virulence factors that otherwise impair DNA repair systems and thus contribute to carcinogenesis [37, 38]. Indeed, human studies profiling the gastric microbiota in *H. pylori* infected and uninfected subjects have demonstrated a wide diversity of bacterial phylotypes in the stomach [39, 40]. A small number of gastric cancer patients were found to be colonized with low numbers of *H. pylori* and significantly, bacteria from 5 other bacterial phyla [23]. The significance of these initial observations warrants further epidemiologic studies in humans and in animal models such as INS-GAS mice where genetic and environmental variability inherent in human subjects can be minimized.

Notably ASF 361 (*Lactobacillus* sp.) colonized the stomach of *H. pylori* infected and *H. polygyrus* co-infected mice at higher levels than control mice. Others have shown that *H. polygyrus* infection in C57BL/6 mice increased the abundance of *Lactobacillaceae* in the ileum [24]. In combination with hypochlorhydria known to develop in INS-GAS mice [19,

25], increased ASF 361 colonization in the stomach may in part be attributable to the relative oxygen resistance of ASF 361 compared to the other obligate anaerobic ASF [30]. Gastric colonization with 3 of 4 ASF were not increased in helminth co-infected mice, coincident with elevated numbers of regulatory T cells and less gastric atrophy and dysplasia. These findings evoke a putative mechanism involving helminth-mediated, regulatory T cell preservation of parietal cell mass and maintenance of colonization resistance of the acidic stomach to lower bowel microflora.

The natural niche for *H. polygyrus* is the duodenum of the mouse, but its impact on host physiology and immune responses are systemic. *H. polygyrus* infection increases permeability of the colonic mucosal barrier [41], induces regulatory T cells [42] and the helminth is known to be immunosuppressive in a variety of inflammation models [11, 32, 43-45] that clearly point to a mechanism involving immune regulation [46]. *H. polygyrus* stimulates innate [44, 47] as well as cell-mediated and humoral immune responses [41]. The *H. polygyrus* re-infection protocol used in this study is designed to maintain a Th2-biased immune response but also models chronic exposure of children to helminths who have received periodic anthelmintic therapy. This reinfection with *H. polygyrus* may also have contributed to duodenitis in response to degenerate *H. polygyrus* larvae and adult worms. As this lesion was observed in *H. polygyrus* infected mice irrespective of *H. pylori* co-infection or severity of gastritis, the significance may be limited except the same lesion may develop in children living in low socioeconomic conditions where parasitism constitutes a significant morbidity in addition to endemic *H. pylori* infection. Alternatively, INS-GAS mice infected with *H. pylori* or co-infected with *H. polygyrus* developed similar, but very robust IL-17, IFN $\gamma$ , TNF $\alpha$  and iNOS responses in gastric tissues with low expression of anti-inflammatory TGF $\beta$  and IL-10 responses and minimal IL-13 expression, suggesting concurrent duodenitis may have muted the anticipated TH2-like cytokine response to helminths, particularly given the length of co-infection in the current experiment.

The robust Th2-associated inflammatory response and the differentiation of IL-10 producing, FoxP3<sup>+</sup> regulatory T cells [42] and regulatory dendritic cells [48] that result from acute *H. polygyrus* infection are evolutionarily important for expulsion of the parasite from the host or alternatively, for the parasite to establish persistent infection. Compared to low numbers of cells expressing the regulatory T cell marker FoxP3 in uninfected controls and mice infected with *H. polygyrus* alone, FoxP3<sup>+</sup> cell numbers were increased in the gastric mucosa and submucosa of *H. pylori* infected INS-GAS mice and were highest in *H. pylori* and *H. polygyrus* co-infected mice. This suggests that *H. polygyrus* promoted regulatory T cell development in lymph nodes which were then recruited to the inflamed stomach and appear to have preserved parietal cell function and maintained acidic gastric pH. In autoimmune mice [49], regulatory T cells suppressed production of inflammatory cytokines in the stomach and prevented parietal cell loss through release of chemokines which regulated effector T cell trafficking into the stomach.

These results support that *H. pylori*-associated gastric atrophy allow opportunistic colonization of the achlorhydric human stomach with lower bowel microflora and that ongoing gastritis and progression of premalignant lesions may occur despite clearance of *H. pylori* infection when gastric atrophy is irreversible [22]. Our previous studies illustrated the

importance of enteric colonization in promoting *H. pylori*-associated gastric cancer in several INS-GAS mouse models [15][16]. In addition, we reported experimental evidence for this concept when INS-GAS mice underwent antibiotic eradication of *H. pylori*, and likely other microbiota that may have colonized the atrophic gastric epithelium, had reduced gastric cancer risk in a time-dependent manner [27, 50]. Rodent models of *Helicobacter* and helminth co-infection have reproduced epidemiologic observations of lower life-time risk for gastric adenocarcinoma in *H. pylori* infected humans living under heavy environmental exposure to parasites, particularly in young children who commonly acquire *H. pylori* and helminths concurrently [9]. Identifying how helminths impact bacterial colonization of the *H. pylori* infected stomach through immune modulation or other mechanisms could lead to new treatment strategies to reduce malignant sequelae from chronic gastritis in humans.

## Acknowledgments

We thank Melissa Mobley and Amanda Potter who performed the necropsies and sample collection. Supported in part by RO1-CA67529, R01DK052413, PO1CA26731, P01 CA028842, P30ESO2109, R01DK065075 (JGF) and R01DK082427 (HNS) from the National Institutes of Health.

## References

1. Correa P, Piazuelo MB. The gastric precancerous cascade. *J Dig Dis.* 2012; 13:2–9. [PubMed: 22188910]
2. McLean MH, El-Omar EM. Genetics of inflammation in the gastrointestinal tract and how it can cause cancer. *Recent Results Cancer Res.* 2011; 185:173–183. [PubMed: 21822827]
3. Camargo MC, Goto Y, Zabaleta J, Morgan DR, Correa P, Rabkin CS. Sex hormones, hormonal interventions, and gastric cancer risk: a meta-analysis. *Cancer Epidemiol Biomarkers Prev.* 2012; 21:20–38. [PubMed: 22028402]
4. de Sablet T, Piazuelo MB, Shaffer CL, Schneider BG, Asim M, Chaturvedi R, Bravo LE, Sicinski LA, Delgado AG, Mera RM, Israel DA, Romero-Gallo J, Peek RM Jr, Cover TL, Correa P, Wilson KT. Phylogeographic origin of *Helicobacter pylori* is a determinant of gastric cancer risk. *Gut.* 2011; 60:1189–1195. [PubMed: 21357593]
5. Fox JG, Dangler CA, Taylor NS, King A, Koh TJ, Wang TC. High-salt diet induces gastric epithelial hyperplasia and parietal cell loss, and enhances *Helicobacter pylori* colonization in C57BL/6 mice. *Cancer Res.* 1999; 59:4823–4828. [PubMed: 10519391]
6. Rogers AB, Taylor NS, Whary MT, Stefanich ED, Wang TC, Fox JG. *Helicobacter pylori* but not high salt induces gastric intraepithelial neoplasia in B6129 mice. *Cancer Res.* 2005; 65:10709–10715. [PubMed: 16322215]
7. Lemke LB, Ge Z, Whary MT, Feng Y, Rogers AB, Muthupalani S, Fox JG. Concurrent *Helicobacter bilis* infection in C57BL/6 mice attenuates proinflammatory *H. pylori*-induced gastric pathology. *Infect Immun.* 2009; 77:2147–2158. [PubMed: 19223483]
8. Ge Z, Feng Y, Muthupalani S, Eurell LL, Taylor NS, Whary MT, Fox JG. Coinfection with enterohepatic *Helicobacter* species can ameliorate or promote *Helicobacter pylori*-induced gastric pathology in C57BL/6 mice. *Infect Immun.* 2011; 79:3861–3871. [PubMed: 21788386]
9. Whary MT, Sundina N, Bravo LE, Correa P, Quinones F, Caro F, Fox JG. Intestinal helminthiasis in Colombian children promotes a Th2 response to *Helicobacter pylori*: possible implications for gastric carcinogenesis. *Cancer Epidemiol Biomarkers Prev.* 2005; 14:1464–1469. [PubMed: 15941957]
10. Ek C, Whary MT, Ihrig M, Bravo LE, Correa P, Fox JG. Serologic evidence that ascaris and toxoplasma infections impact inflammatory responses to *Helicobacter pylori* in Colombians. *Helicobacter.* 2012; 17:107–115. [PubMed: 22404440]

11. Fox JG, Beck P, Dangler CA, Whary MT, Wang TC, Shi HN, Nagler-Anderson C. Concurrent enteric helminth infection modulates inflammation and gastric immune responses and reduces helicobacter-induced gastric atrophy. *Nat Med.* 2000; 6:536–542. [PubMed: 10802709]
12. Martin HR, Shakya KP, Muthupalani S, Ge Z, Klei TR, Whary MT, Fox JG. *Brugia filariasis* differentially modulates persistent *Helicobacter pylori* gastritis in the gerbil model. *Microbes Infect.* 2010; 12:748–758. [PubMed: 20685294]
13. Kuipers EJ. Proton pump inhibitors and gastric neoplasia. *Gut.* 2006; 55:1217–1221. [PubMed: 16905689]
14. Fox J, Sheh A. The role of the gastrointestinal microbiome in *Helicobacter pylori* pathogenesis. *Gut Microbes.* 2013; 4
15. Lofgren JL, Whary MT, Ge Z, Muthupalani S, Taylor NS, Mobley M, Potter A, Varro A, Eibach D, Suerbaum S, Wang TC, Fox JG. Lack of commensal flora in *Helicobacter pylori*-infected INS-GAS mice reduces gastritis and delays intraepithelial neoplasia. *Gastroenterology.* 2011; 140:210–220. [PubMed: 20950613]
16. Lertpiriyapong K, Whary MT, Muthupalani S, Lofgren JL, Gamazon ER, Feng Y, Ge Z, Wang TC, Fox JG. Gastric colonisation with a restricted commensal microbiota replicates the promotion of neoplastic lesions by diverse intestinal microbiota in the *Helicobacter pylori* INS-GAS mouse model of gastric carcinogenesis. *Gut.* 2014; 63:54–63. [PubMed: 23812323]
17. Fox JG, Rogers AB, Ihrig M, Taylor NS, Whary MT, Dockray G, Varro A, Wang TC. *Helicobacter pylori*-associated gastric cancer in INS-GAS mice is gender specific. *Cancer Res.* 2003; 63:942–950. [PubMed: 12615707]
18. Sheh A, Lee CW, Masumura K, Rickman BH, Nohmi T, Wogan GN, Fox JG, Schauer DB. Mutagenic potency of *Helicobacter pylori* in the gastric mucosa of mice is determined by sex and duration of infection. *Proc Natl Acad Sci U S A.* 2010; 107:15217–15222. [PubMed: 20699385]
19. Wang TC, Dangler CA, Chen D, Goldenring JR, Koh T, Raychowdhury R, Coffey RJ, Ito S, Varro A, Dockray GJ, Fox JG. Synergistic interaction between hypergastrinemia and *Helicobacter* infection in a mouse model of gastric cancer. *Gastroenterology.* 2000; 118:36–47. [PubMed: 10611152]
20. Boivin GP, Washington K, Yang K, Ward JM, Pretlow TP, Russell R, Besselsen DG, Godfrey VL, Doetschman T, Dove WF, Pitot HC, Halberg RB, Itzkowitz SH, Groden J, Coffey RJ. Pathology of mouse models of intestinal cancer: consensus report and recommendations. *Gastroenterology.* 2003; 124:762–777. [PubMed: 12612914]
21. Hagiwara T, Mukaisho K, Nakayama T, Sugihara H, Hattori T. Long-term proton pump inhibitor administration worsens atrophic corpus gastritis and promotes adenocarcinoma development in Mongolian gerbils infected with *Helicobacter pylori*. *Gut.* 2011; 60:624–630. [PubMed: 21097844]
22. Fox JG, Kuipers EJ. Long-term proton pump inhibitor administration, *H. pylori* and gastric cancer: lessons from the gerbil. *Gut.* 2011; 60:567–568. [PubMed: 21330575]
23. Dicksved J, Lindberg M, Rosenquist M, Enroth H, Jansson JK, Engstrand L. Molecular characterization of the stomach microbiota in patients with gastric cancer and in controls. *J Med Microbiol.* 2009; 58:509–516. [PubMed: 19273648]
24. Walk ST, Blum AM, Ewing SA, Weinstock JV, Young VB. Alteration of the murine gut microbiota during infection with the parasitic helminth *Heligmosomoides polygyrus*. *Inflamm Bowel Dis.* 2010; 16:1841–1849. [PubMed: 20848461]
25. Wang TC, Koh TJ, Varro A, Cahill RJ, Dangler CA, Fox JG, Dockray GJ. Processing and proliferative effects of human progastrin in transgenic mice. *J Clin Invest.* 1996; 98:1918–1929. [PubMed: 8878444]
26. Shi HN, Scott ME, Koski KG, Boulay M, Stevenson MM. Energy restriction and severe zinc deficiency influence growth, survival and reproduction of *Heligmosomoides polygyrus* (Nematoda) during primary and challenge infections in mice. *Parasitology.* 1995; 110(Pt 5):599–609. [PubMed: 7596643]
27. Lee CW, Rickman B, Rogers AB, Muthupalani S, Takaishi S, Yang P, Wang TC, Fox JG. Combination of sulindac and antimicrobial eradication of *Helicobacter pylori* prevents progression

- of gastric cancer in hypergastrinemic INS-GAS mice. *Cancer Res.* 2009; 69:8166–8174. [PubMed: 19826057]
28. Schlemper RJ, Kato Y, Stolte M. Diagnostic criteria for gastrointestinal carcinomas in Japan and Western countries: proposal for a new classification system of gastrointestinal epithelial neoplasia. *J Gastroenterol Hepatol.* 2000; 15:G49–57. Suppl. [PubMed: 11100994]
  29. Rogers AB, Cormier KS, Fox JG. Thiol-reactive compounds prevent nonspecific antibody binding in immunohistochemistry. *Lab Invest.* 2006; 86:526–533. [PubMed: 16534499]
  30. Sarma-Rupavtarm RB, Ge Z, Schauer DB, Fox JG, Polz MF. Spatial distribution and stability of the eight microbial species of the altered Schaedler flora in the mouse gastrointestinal tract. *Appl Environ Microbiol.* 2004; 70:2791–2800. [PubMed: 15128534]
  31. Ge Z, Feng Y, Taylor NS, Ohtani M, Polz MF, Schauer DB, Fox JG. Colonization dynamics of altered Schaedler flora is influenced by gender, aging, and *Helicobacter hepaticus* infection in the intestines of Swiss Webster mice. *Appl Environ Microbiol.* 2006; 72:5100–5103. [PubMed: 16820515]
  32. Shi HN, Ingui CJ, Dodge I, Nagler-Anderson C. A helminth-induced mucosal Th2 response alters nonresponsiveness to oral administration of a soluble antigen. *J Immunol.* 1998; 160:2449–2455. [PubMed: 9498789]
  33. Dewhirst FE, Chien CC, Paster BJ, Ericson RL, Orcutt RP, Schauer DB, Fox JG. Phylogeny of the defined murine microbiota: altered Schaedler flora. *Appl Environ Microbiol.* 1999; 65:3287–3292. [PubMed: 10427008]
  34. Fox JG, Wang TC. Inflammation, atrophy, and gastric cancer. *J Clin Invest.* 2007; 117:60–69. [PubMed: 17200707]
  35. Whary MT, Danon SJ, Feng Y, Ge Z, Sundina N, Ng V, Taylor NS, Rogers AB, Fox JG. Rapid onset of ulcerative typhlocolitis in B6.129P2-IL10tm1Cgn (IL-10<sup>-/-</sup>) mice infected with *Helicobacter troglodytes* is associated with decreased colonization by altered Schaedler's flora. *Infect Immun.* 2006; 74:6615–6623. [PubMed: 16982822]
  36. Zavros Y, Rieder G, Ferguson A, Samuelson LC, Merchant JL. Genetic or chemical hypochlorhydria is associated with inflammation that modulates parietal and G-cell populations in mice. *Gastroenterology.* 2002; 122:119–133. [PubMed: 11781287]
  37. Touati E. When bacteria become mutagenic and carcinogenic: lessons from *H. pylori*. *Mutat Res.* 2010; 703:66–70. [PubMed: 20709622]
  38. Meira LB, Bugni JM, Green SL, Lee CW, Pang B, Borenshtein D, Rickman BH, Rogers AB, Moroski-Erkul CA, McFaline JL, Schauer DB, Dedon PC, Fox JG, Samson LD. DNA damage induced by chronic inflammation contributes to colon carcinogenesis in mice. *J Clin Invest.* 2008; 118:2516–2525. [PubMed: 18521188]
  39. Bik EM, Eckburg PB, Gill SR, Nelson KE, Purdom EA, Francois F, Perez-Perez G, Blaser MJ, Relman DA. Molecular analysis of the bacterial microbiota in the human stomach. *Proc Natl Acad Sci U S A.* 2006; 103:732–737. [PubMed: 16407106]
  40. Sheh A, Piazzuelo MB, Wilson KT, Correa P, Fox JG. Draft genome sequences of *Helicobacter pylori* strains isolated from regions of low and high gastric cancer risk in Colombia. *Genome Announcements.* 2013; 1
  41. Su CW, Cao Y, Kaplan J, Zhang M, Li W, Conroy M, Walker WA, Shi HN. Duodenal helminth infection alters barrier function of the colonic epithelium via adaptive immune activation. *Infect Immun.* 2011; 79:2285–2294. [PubMed: 21444669]
  42. Grainger JR, Smith KA, Hewitson JP, McSorley HJ, Hargus Y, Filbey KJ, Finney CA, Greenwood EJ, Knox DP, Wilson MS, Belkaid Y, Rudensky AY, Maizels RM. Helminth secretions induce de novo T cell Foxp3 expression and regulatory function through the TGF-beta pathway. *J Exp Med.* 2010; 207:2331–2341. [PubMed: 20876311]
  43. Weng M, Huntley D, Huang IF, Foye-Jackson O, Wang L, Sarkissian A, Zhou Q, Walker WA, Cherayil BJ, Shi HN. Alternatively activated macrophages in intestinal helminth infection: effects on concurrent bacterial colitis. *J Immunol.* 2007; 179:4721–4731. [PubMed: 17878371]
  44. Hang L, Setiawan T, Blum AM, Urban J, Stoyanoff K, Arihiro S, Reinecker HC, Weinstock JV. *Heligmosomoides polygyrus* infection can inhibit colitis through direct interaction with innate immunity. *J Immunol.* 2010; 185:3184–3189. [PubMed: 20702728]

45. Shi M, Wang A, Prescott D, Waterhouse CC, Zhang S, McDougall JJ, Sharkey KA, McKay DM. Infection with an intestinal helminth parasite reduces Freund's complete adjuvant-induced monoarthritis in mice. *Arthritis Rheum.* 2011; 63:434–444. [PubMed: 20967852]
46. Smith KA, Hochweller K, Hammerling GJ, Boon L, MacDonald AS, Maizels RM. Chronic helminth infection promotes immune regulation in vivo through dominance of CD11c<sup>lo</sup>CD103<sup>-</sup> dendritic cells. *J Immunol.* 2011; 186:7098–7109. [PubMed: 21576507]
47. Sutton TL, Zhao A, Madden KB, Elfrey JE, Tuft BA, Sullivan CA, Urban JF Jr, Shea-Donohue T. Anti-Inflammatory mechanisms of enteric *Heligmosomoides polygyrus* infection against trinitrobenzene sulfonic acid-induced colitis in a murine model. *Infect Immun.* 2008; 76:4772–4782. [PubMed: 18644879]
48. Li Z, Liu G, Chen Y, Liu Y, Liu B, Su Z. The phenotype and function of naturally existing regulatory dendritic cells in nematode-infected mice. *Int J Parasitol.* 2011; 41:1129–1137. [PubMed: 21827765]
49. Nguyen TL, Sullivan NL, Ebel M, Teague RM, DiPaolo RJ. Antigen-specific TGF-beta-induced regulatory T cells secrete chemokines, regulate T cell trafficking, and suppress ongoing autoimmunity. *J Immunol.* 2011; 187:1745–1753. [PubMed: 21746962]
50. Lee CW, Rickman B, Rogers AB, Ge Z, Wang TC, Fox JG. *Helicobacter pylori* eradication prevents progression of gastric cancer in hypergastrinemic INS-GAS mice. *Cancer Res.* 2008; 68:3540–3548. [PubMed: 18441088]

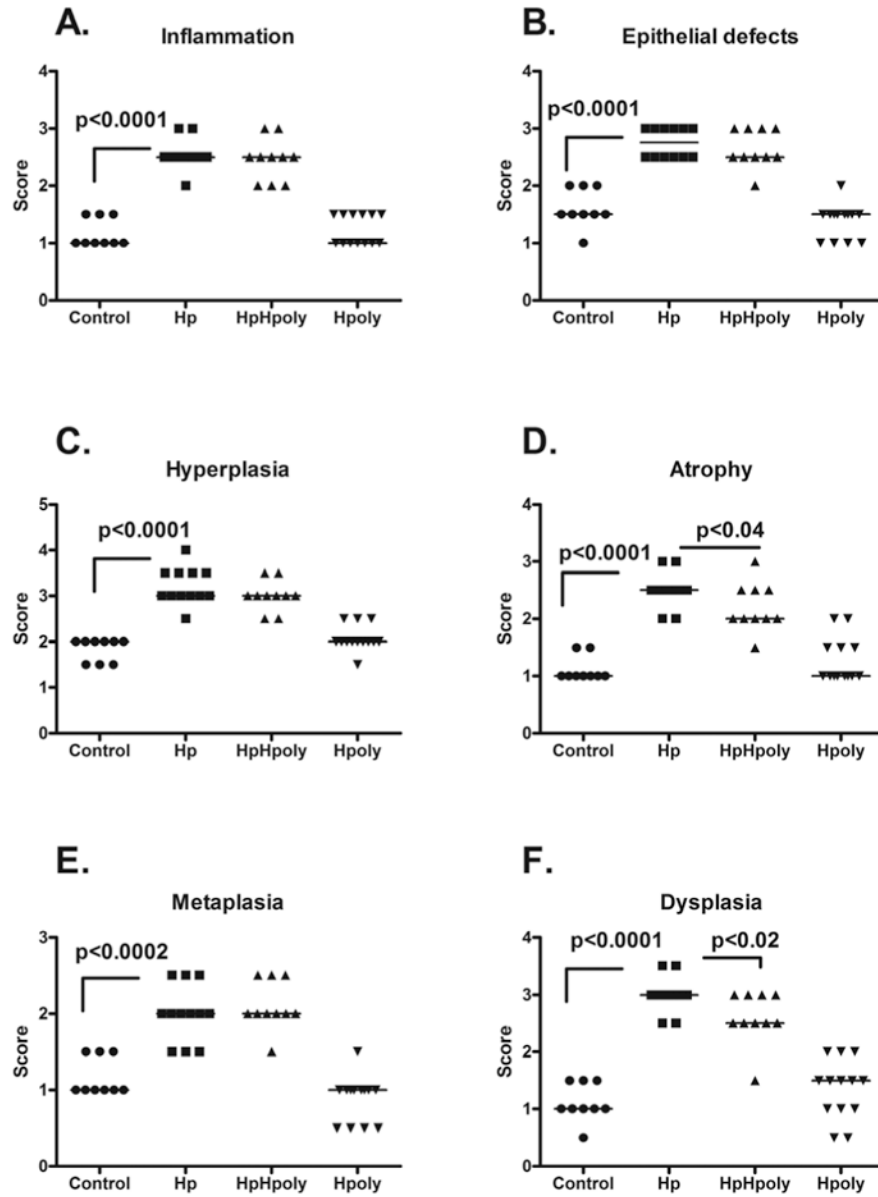


**Fig. 1.** Median scores for gastric inflammation, epithelial defects, epithelial (foveolar/glandular hyperplasia), gastric atrophy, pseudopyloric metaplasia and dysplasia. At 5 months post infection (mpi) with *H. pylori* (Hp)(n=12), median scores for all features were significantly higher than controls (n=9) or mice infected with *H. polygyrus* (Hpoly) (n=13) alone. Compared to Hp infected mice, gastric atrophy and dysplasia were significantly less severe in *H. pylori* and *H. polygyrus* co-infected mice (HpHpoly) and the incidence of GIN was lower (n=10).



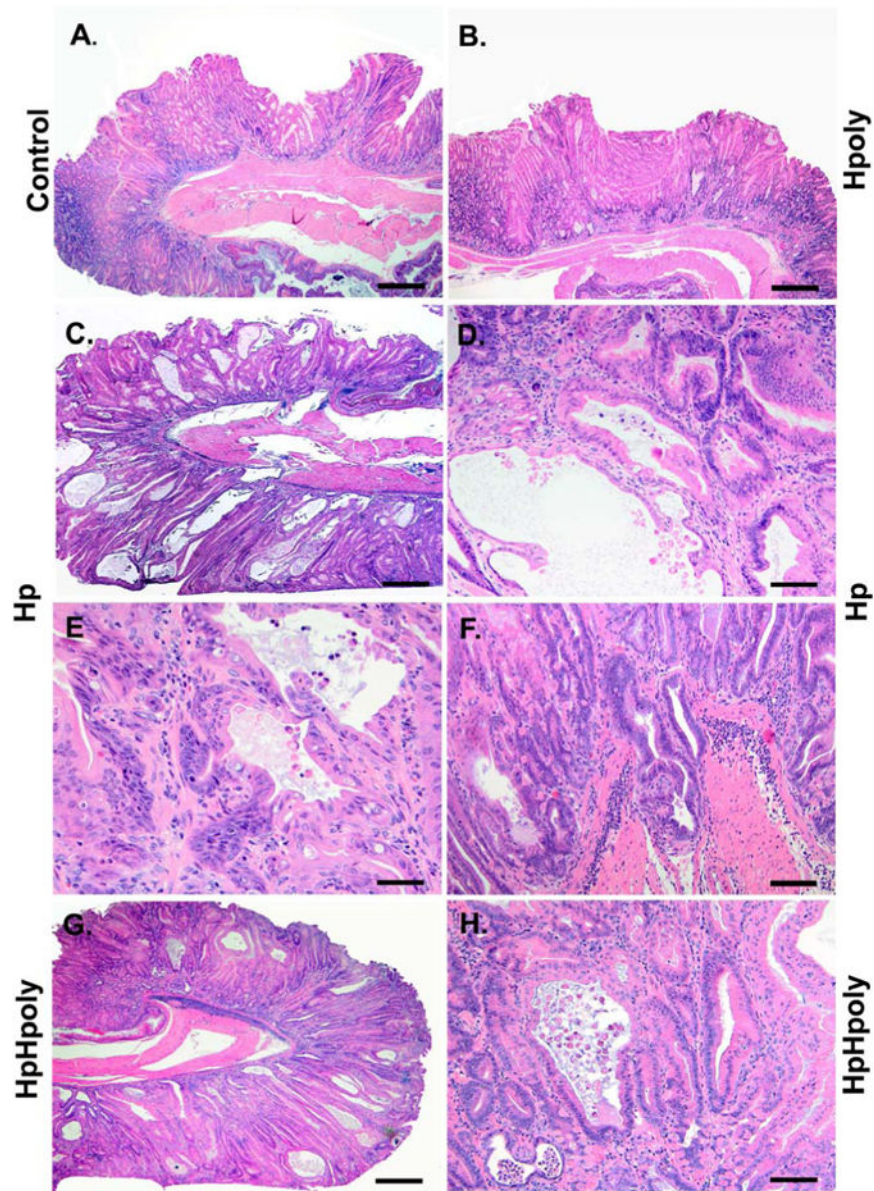


**Fig. 2.** **A-H.** (A) Representative hematoxylin and eosin stained image of the gastric corpus from a control, uninfected male INS-GAS mouse necropsied at a time equivalent to 5 months post infection (mpi) for *H. pylori*. Bar = 400  $\mu$ M. (B) Gastric corpus from a male INS-GAS mouse infected with *H. polygyrus* 6 mpi, equivalent to 5 mpi for *H. pylori*. The extent of epithelial hyperplasia and oxyntic loss was low to moderate with sparse inflammation and minimal dysplasia and is similar to the uninfected control male INS-GAS mice in Panel A. Bar = 400  $\mu$ M. (C-E) Representative low and high power magnification of hematoxylin and eosin stained images of the gastric corpus from a male INS-GAS mouse 5 mpi with *H. pylori*. In the low magnification image (C) (Bar = 400  $\mu$ M), there is severe diffuse pathomorphological alterations in the corpus characterized by significant distortion of normal gastric glandular columnar architecture with numerous cystic, dilated glands,

prominent foveolar and glandular epithelial hyperplasia, metaplasia, oxyntic loss or atrophy, with mild to moderate inflammation in the mucosa and submucosa. This lesion has high grade dysplasia with rare invasive glands in the lamina propria consistent with gastrointestinal intramucosal carcinoma as well as partially herniated glands (lined by peripheral muscularis mucosa) in the submucosa. A high magnification focus of the proximal corpus as shown in **(D)** (Bar = 75  $\mu$ M) revealing loss of glandular columnar orientation with arborizing, dysplastic and ectatic atypical glands containing intraluminal cellular ghosts against a background of distinct stromal inflammation. **(E)** is a higher magnification image (Bar = 40  $\mu$ M) showing dysplastic glands with cellular atypia, necrosis and apoptosis of cells that are sloughing into the lumen, loss of basal lining and invasion of dysplastic epithelial cells into the lamina propria, thus fulfilling the histological criteria for gastrointestinal intramucosal carcinoma. A high magnification image **(F)** (Bar = 75  $\mu$ M) of the proximal corpus from a male INS-GAS mouse 5 mpi with *H. pylori* showing herniation of a group of dysplastic gastric glands through the muscularis mucosa into the submucosa in a region of submucosal inflammation. **(G)** Proximal corpus from a male INS-GAS mouse 5 mpi with *H. pylori* and *H. polygyrus* at low magnification (Bar = 400  $\mu$ M). Inflammation and hyperplasia remain significant but there is a slight reduction in the overall severity of epithelial distortion/defects, glandular metaplasia, oxyntic atrophy and extent of dysplasia as compared to the age-matched *H. pylori* monoinfected INS-GAS as shown in **(C)**. **(H)** Higher magnification image from **(G)** depicting an area of glandular metaplasia, dysplastic and ectatic glands with intraluminal cellular debris but absence of lamina propria invasion (Bar = 75  $\mu$ M).

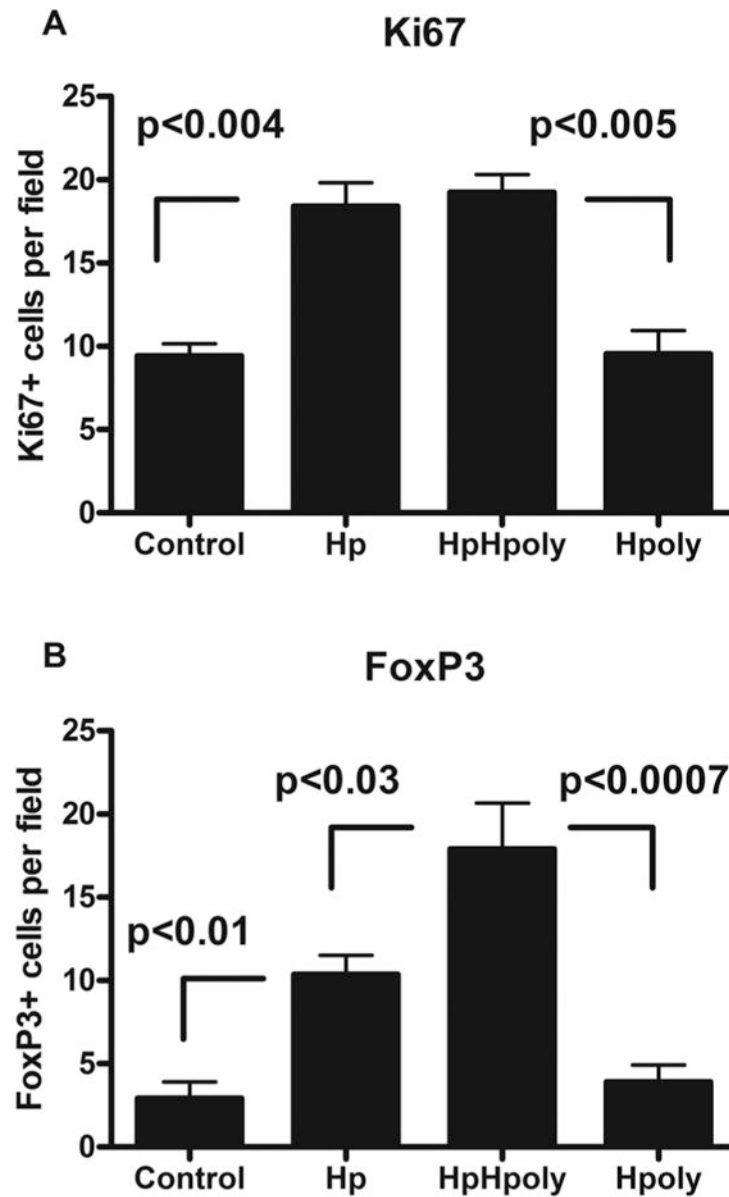


**Fig. 3.**

The gastric corpus from 5 to 7 mice per group were labeled by immunohistochemistry to enumerate Ki67 (**A**) and FoxP3 positive cells (**B**). Compared to baseline values from uninfected control INS-GAS mice, (**A**) the mean ( $\pm$  St. Dev.) Ki67 labeling index, reflecting epithelial (foveolar/glandular) hyperplasia, was significantly higher in mice infected with *H. pylori* (Hp). The number of Ki67+ cells was similarly high in mice co-infected with *H. pylori* and *H. polygyrus* (HpHpoly). (**B**) the mean ( $\pm$  St. Dev.) FoxP3 labeling index, reflecting regulatory T cells, was significantly higher in mice infected with *H. pylori* (Hp).

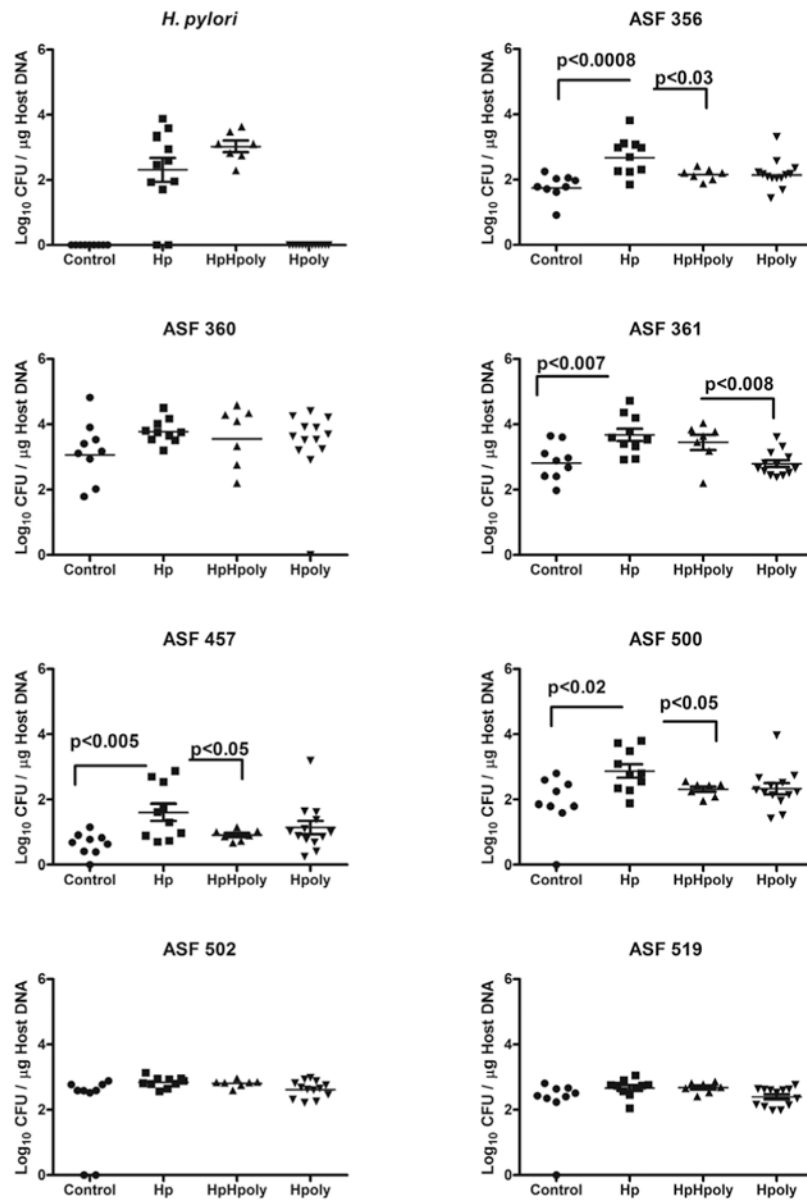


**Fig. 4.** Geometric means for gastric colonization of *H. pylori* and ASF by quantitative PCR (qPCR). *H. polygyrus* co-infection (HpHpoly) had minimal impact on *H. pylori* colonization. Gastric colonization levels of 4 ASF were increased in *H. pylori* infected mice (Hp) and helminth co-infection prevented increased colonization of 3 of these ASF.

**Table 1**

Quantitative PCR for mRNA expression in gastric tissues at 5 months post *H. pylori* infection: Ranked by fold-change in response to *H. pylori* infection (Mean  $\pm$  StDev.).

|              | Infection Status |                  |  |                     |
|--------------|------------------|------------------|--|---------------------|
|              | Control          | <i>H. pylori</i> | <i>H. pylori</i> & <i>H. polygyrus</i> | <i>H. polygyrus</i> |
| IL-17F       | 0 $\pm$ 2.2      | 112 $\pm$ 1.5*   | 87 $\pm$ 1.4*                          | -0.6 $\pm$ 1.7      |
| IFN $\gamma$ | 0 $\pm$ 2.0      | 105 $\pm$ 1.8*   | 126 $\pm$ 2.1*                         | -0.3 $\pm$ 1.7      |
| IL-17A       | 0 $\pm$ 1.3      | 28 $\pm$ 1.4*    | 29 $\pm$ 1.3*                          | 0.3 $\pm$ 1.3       |
| TNF $\alpha$ | 0 $\pm$ 1.3      | 18 $\pm$ 1.6*    | 16 $\pm$ 0.2*                          | 0.01 $\pm$ 1.4      |
| iNOS         | 0 $\pm$ 1.3      | 15 $\pm$ 2.2*    | 15 $\pm$ 1.8*                          | -0.1 $\pm$ 1.5      |
| TGF $\beta$  | 0 $\pm$ 1.3      | 3.3 $\pm$ 1.2**  | 3.6 $\pm$ 1.1**                        | 0.1 $\pm$ 1.4       |
| IL-1 $\beta$ | 0 $\pm$ 1.5      | 1.4 $\pm$ 1.5**  | 1.1 $\pm$ 1.4**                        | -0.2 $\pm$ 1.4      |
| IL-10        | 0 $\pm$ 1.2      | 1.2 $\pm$ 1.3**  | 1.1 $\pm$ 1.2**                        | 0.01 $\pm$ 1.3      |
| IL-13        | 0 $\pm$ 2.1      | -0.3 $\pm$ 0.3   | -0.1 $\pm$ 1.6                         | 0.6 $\pm$ 0.1       |

\* p<0.0001;

\*\* p<0.05 compared to controls.